Journal of Achievements in Materials and Manufacturing Engineering
VOLUME 49
ISSUE 2
December
2011

Efficiency of the computer tomography algorithms in examination of the internal structure of materials with non-transparent elements by using the incomplete information

R. Grzymkowski, E. Hetmaniok, M. Pleszczyński*
Institute of Mathematics, Silesian University of Technology,
ul. Kaszubska 23, 44-100 Gliwice, Poland
* Corresponding author: E-mail address: mariusz.pleszczynski@polsl.pl

Received 07.10.2011; published in revised form 01.12.2011

Analysis and modelling

ABSTRACT

Purpose: of this paper: The effectiveness of computer tomography algorithms applied for reconstructing the internal structure of objects containing the non-transparent elements is discussed, in conditions of the incomplete information about the examined object.
Design/methodology/approach: Problem of the internal structure examination of an object with non-transparent elements, without its destruction, is considered by means of the classical and non-classical algebraic algorithms of computer tomography used in standard approaches and in cases of incomplete projection data.
Findings: Computer tomography algorithms, known from literature and designed by the authors, are tested in solving the problems of reconstructing the discrete objects of high contrast with non-transparent elements, with regard to their precision, convergence and utility. Carried out research indicate that the chaotic algorithms are more efficient, for the same values of parameters, in comparison with the corresponding classical algorithms.
Practical implications: Problems considered in the paper can arise in some technical issues, for example, in exploring the coal interlayers in looking for the compressed gas reservoirs which can be dangerous for the people's life and health, in which application of the standard algorithms of computer tomography is impossible for some reasons (like size of the examined object, its localization or its accessibility).
Originality/value: In the paper the originally designed by the authors reconstruction algorithms are presented which appear to be more effective than the standard algebraic algorithms adapted for solving problems with the incomplete projection data.
Keywords: Numerical techniques; Computer tomography; Parallel algorithms; Chaotic algorithms

Reference to this paper should be given in the following way:
R. Grzymkowski, E. Hetmaniok, M. Pleszczyński, Efficiency of the computer tomography algorithms in examination of the internal structure of materials with non-transparent elements by using the incomplete information, Journal of Achievements in Materials and Manufacturing Engineering 49/2 (2011) 285-298.

© Copyright by International OCSCO World Press. All rights reserved. 2011

1. Introduction

Methods of computer tomography can be used, not only in medicine but also in wide class of technical problems, in every case when the examination of internal structure of an object, without its destruction, is needed. Computer tomography algorithms can be divided into two groups: analytic and algebraic algorithms. In this elaboration we will consider the algebraic algorithms only.

Let $f(x,y)$ be a function representing the spatial distribution of some physical parameter. Then, as a projection we define the line integral:

$$p_L = \int_L f(x,y)dL, \tag{1}$$

where L is an interval in the plane connecting the source of beam radiation with the detector. The projection is usually obtained from real physical measurements.

From mathematical point of view the problem of reconstructing the object from projections consists in finding an unknown function $f(x,y)$ by means of a given set of projections $\boldsymbol{p_L}$ for all L. It is theoretically possible to reconstruct the function $f(x,y)$ from the set $\boldsymbol{p_L}$ by means of the Radon inversion formula [20]. However, in practice only a discrete set of projection data for a limited number of rays is given. Moreover, since the projection data are obtained by real physical measurements, they are perturbed by the random errors. Another problem is that in many practical applications the projection data may not be available at each direction and its number may be very limited. In this case we say that we have a reconstruction problem with incomplete projection data. In particular, such kind of problems arises in mineral industries and engineering geophysics connected with acid mine drainage, the stability of mine workers, mineral exploration and others [1,2]. Next problem which can appear in practical situations is the presence of the non-transparent elements in examined objects. In mining industry the non-transparent elements could be, for example, the objects lying in the coal interlayer and having strictly higher capacity than coal to absorb energy, as well as stones or compressed gas, usually present in coal interlayer. With all the mentioned problems, with reference to computer tomography, will we deal in the current paper.

Let us notice that the energy lost by the given ray is equal to the sum of energies lost in the particular pixels occurring in the trajectory of this ray, and that every pixel absorbs the portion of energy which is proportional to the value of function f in this pixel and to the length of path passed by the ray to this pixel. Values of the absorption coefficients are unknown, whereas regions of the intersections of rays and pixels can be determined by knowing the discretization density and the equations of lines containing those rays. There are also known the initial and terminal values of the rays energies, so difference between them in consequence, which means that all of the projection values are known. Those pieces of information give the basis for formulating the system of linear equations. Problem of computer tomography, determined in this way, consists in solving the following system of linear equations:

$$\mathbf{A}\cdot\mathbf{x} = \mathbf{p}, \tag{2}$$

where:

$\mathbf{A} = (a_{ij}) \in \mathbf{R}^{m,n}$ - matrix of coefficients;

$\mathbf{x} = (x_1, x_2, ..., x_n)^T \in \mathbf{R}^n$ - vector of unknown elements;

$\mathbf{p} = (p_1, p_2, ..., p_m) \in \mathbf{R}^m$ - vector of projection.

Method of solution of the above system of equations is equivalent to the considered algebraic algorithms. In the next two sections the approaches appropriate for the classical and non-classical algebraic algorithms of computer tomography will be presented.

More detailed description of the considered problem with the figures explaining the essence of the problem can be found in [13,17].

2. Classical algorithms

We consider the system (2) of algebraic linear equations, constructed in the way described in the previous section. For solving this problem we describe three approaches corresponding with three algorithms [3,4].

2.1. ART algorithm

We will use the following notations:

$$\mathbf{P}_i(\mathbf{x}) = \mathbf{x} - \frac{(\mathbf{a}^i, \mathbf{x}) - p_i}{\left\|\mathbf{a}^i\right\|^2}\mathbf{a}^i, \tag{3}$$

$$\mathbf{P}_i^{\omega} = (1-\omega)\mathbf{I} + \omega\mathbf{P}_i, \tag{4}$$

where $\mathbf{a}^i$ is the *i-th* row of the matrix $\mathbf{A}$, $0<\omega<2$ denotes the relaxation parameter and $\mathbf{I}$ refers to the identity matrix. Then we proceed in the following way:

1. $\mathbf{x}^{(0)} \in \mathbf{R}^n$ is an arbitrary vector;

2. *(k+1)-th* vector is received by the formula:

$$\mathbf{x}^{(k+1)} = \mathbf{P}_i^{\omega_k}\mathbf{x}^{(k)} \quad (i = 1,2,...,m), \tag{5}$$

where $\mathbf{P}_i^{\omega_k}$ is an operator defined by means of (4), ω_k denotes the relaxation parameter and $i(k)=k(\mathrm{mod}\ m)+1$.

The convergence conditions of the ART algorithm are proved in [5].

2.2. ART-3 algorithm

Let us denote:

$$\mathbf{P}_i(\mathbf{x}) = \mathbf{x} - \frac{((\mathbf{a}^i, \mathbf{x}) - p_i - \varepsilon_i)^+ - (p_i - \varepsilon_i - (\mathbf{a}^i, \mathbf{x}))^+}{\left\|\mathbf{a}^i\right\|^2}\mathbf{a}^i, \tag{6}$$

where:

$$s^{+} = \begin{cases} s, & \text{if } s \geq 0; \\ 0, & \text{otherwise} \end{cases} \tag{7}$$

and

$$\mathbf{P}_i^{\omega} = (1-\omega)\mathbf{I} + \omega\mathbf{P}_i, \tag{8}$$

where $\mathbf{a}^i$ is the *i-th* row of the matrix **A**, 0<ω<2 denotes the relaxation parameter and **I** refers to the identity matrix. Then we make the following steps:

1. $\mathbf{x}^{(0)} \in \mathbf{R}^n$ is an arbitrary vector;

2. *(k+1)-th* vector is received by the formula:

$$\mathbf{P}_i^{\omega} = (1-\omega)\mathbf{I} + \omega\mathbf{P}_i, \tag{9}$$

where $\mathbf{P}_i^{\omega_k}$ is an operator defined by means of relations (6) and (8), ω_k denotes the relaxation parameter and $i(k)=k(\text{mod } m)+1$. In this case, vector $\mathbf{e} = (\varepsilon_1, \varepsilon_2, ..., \varepsilon_m)$ refers to the vector of errors which noise the projections **p**. Then, instead of solving the system of equations (2) we solve the system of inequalities of the form:

$$\mathbf{p} - \mathbf{e} \leq \mathbf{A} \cdot \mathbf{x} \leq \mathbf{p} + \mathbf{e}.$$

2.3. MART algorithm

The MART algorithm is the multiplicative algorithm, on opposite to the ART and ART-3 algorithms which are additive. The MART algorithm can be presented in following iterative form:

1. $0 < \mathbf{x}^{(0)} \in \mathbf{R}^n$ is an arbitrary vector;

2. *(k+1)-th* vector is received by the formula:

$$x_j^{(k+1)} = \left(\frac{p_i}{(\mathbf{a}^{i(k)}, \mathbf{x}^{(k)})} \right)^{\lambda_k^i a_{ij}} x_j^{(k)}, \tag{10}$$

where $\mathbf{a}^i$ is the *i-th* row of the matrix **A**, λ denotes the relaxation parameter and *i=k(mod m)+1.*

In this algorithm the relaxation algorithm can be constant or variable and convergence of this algorithm is determined by theorem presented in [13]. According to this theorem, if the system of equations (2) is not contradictory and for each *i, j, k* the inequality $0 < \lambda_k^i a_{ij} \leq 1$ is true, then the sequence of (10) converges to the solution of the system (2).

3. Non-classical algorithms

Algorithms ART, ART-3 and MART are useful in solving the standard problems as well as in considering the problems of incomplete projection data. However, in cases of the significant limitation of data the convergence of the above algorithms becomes slow. In this section we present some known algorithms and we introduce algorithms designed by the authors for the purpose of speeding up the reconstruction of the examined objects. In the previous considerations, the selection order of the equations in the successive iterations of the algorithms was always the same. It turns out that the order of selection can have a big influence for the speed of algorithm convergence. This conclusion has been taken into account in the asynchronous algorithms, which include the chaotic algorithms [12]. Another approach for increasing the running speed of the algorithm consists in introducing the special type of parallel algorithms and implementing them in the parallel computing systems [6,8,11]. Such kind of process happens by including, in the operation of solving the system of equations, some group of processors working independently and simultaneously, which can significantly reduce the time of determining single iteration. Group of algorithms realising this idea are the block-parallel algorithms. There are two ways of obtaining the parallelism in the algorithm. First approach is the following: the matrix of coefficients is divided into blocks and every block corresponds with one processor, which uses only the rows of matrix contained in this particular block and generates the partial solution. In the next step, the central processor averages the solutions which ends the iteration. Another way for receiving parallelism of the algorithm starts similarly, in dividing the coefficient matrix into blocks corresponding with the processors working independently and simultaneously, but the operations into every single block are executed sequentially. Every successive solution is received as the averaged value of solutions of all blocks.

3.1. Iterative-block algorithms

In practical realization of the parallel algorithms a big number of local processors in the parallel computing structures is required. For the purpose of reducing the number of required local processors we will consider the iterative-block algorithms [10].

Let the matrix **A** and the projection vector **p** be decomposed into *M* subsets according to the condition:

$$\{1,2,...,m\} = H_1 \cup H_2 \cup ... \cup H_M, \tag{11}$$

where $\{1,2,...,m\}$ is the set of indices of the matrix rows and:

$$H_t = \{m_{t-1}+1, m_{t-1}+2, ..., m_t\} \tag{12}$$

for $0 = m_0 < m_1 < ... < m_s = m$.

In the iterative-block algorithm SZB-3, designed by the authors, there are the following steps:

1. $\mathbf{x}^{(0)} \in \mathbf{R}^n$ is an arbitrary vector;

2. *(k+1)-th* vector is received in accordance of the formula:

$$\mathbf{x}^{(k+1)} = \mathbf{C} \sum_{i \in H_{t(k)}} \mathbf{B}_i^k \mathbf{P}_i^{\varpi_k} \mathbf{x}^{(k)}, \tag{13}$$

where $t(k) = k(\text{mod } M) + 1$, $\mathbf{P}_i^{\omega_k}$ is an operator defined with the aid of formulas (6) and (8), $0 < \omega_k < 2$ denotes the relaxation coefficient, **C** is the constraining operator (defined in section 3.3) and $\mathbf{B}_i^k$ describes the matrix of dimension $n \times n$, with the nonnegative elements of the form:

$$\mathbf{B}_i^k = diag\{b_1^{k,i}, b_2^{k,i}, ..., b_n^{k,i}\}, \tag{14}$$

where:

$$b_p^{k,i} = \frac{y_p^{k,i}}{\sum_{i \in H_{t(k)}} y_p^{k,i}}, \tag{15}$$

for $p = 1,2,...,n.$

3.2. Parallel-block algorithms

In the previously considered algorithms the parallel work is executed in every block, whereas the blocks are connected sequentially. In the algorithms presented in this section, operations are executed sequentially in blocks, while the blocks work simultaneously.

Let us decompose the matrix **A** and the projection vector **p** into blocks, according to the formulas (10) and (11). For every block H_i we introduce an operator, denoted by $\boldsymbol{Q}_i$, defined by composing the operators $\mathbf{P}_{m_i}^{\varpi}, \mathbf{P}_{m_i-1}^{\varpi}, ..., \mathbf{P}_{m_{i-1}+1}^{\varpi}$, determined by the conditions (6) and (8), indices of which belong to the block H_i:

$$\mathbf{Q}_i = \mathbf{P}_{m_i}^{\varpi} \mathbf{P}_{m_i-1}^{\varpi} ... \mathbf{P}_{m_{i-1}+1}^{\varpi}. \tag{16}$$

The parallel-block algorithm RB-3, introduced by the authors, runs as follows:

1. $\mathbf{x}^{(0)} \in \mathbf{R}^n$ is an arbitrary vector;
2. *(k+1)-th* vector is received by the formula:

$$\mathbf{x}^{(k+1)} = \sum_{i=1}^{M} \mathbf{B}_i \mathbf{y}^{k+1,i}, \tag{17}$$

where:

$$\mathbf{y}^{k+1,i} = \mathbf{Q}_i \mathbf{x}^{(k)}, \tag{18}$$

$\boldsymbol{Q}_i$ is an operator described by formula (15) and $\boldsymbol{B}_i$ refers to the matrix of dimension $n \times n$ with the nonnegative elements of the form:

$$\mathbf{B}_i = diag\{b_1^i, b_2^i, ..., b_n^i\}, \tag{19}$$

where:

$$b_p^i = \frac{\sum_{s \in H_i} a_{s,p}}{\sum_{i=1}^{M} a_{s,p}}, \tag{20}$$

for $i = 1,2,..., M$ and $p = 1,2,..., n.$

3.3. Chaotic algorithms

The asynchronous algorithms are based on the methods of asynchronous iterations proposed under the name "random relaxations" by D.Chazan and W.Miranker [9], and further developed by G.M.Baudet [7] and M.N.El Tarazi [19] who introduced a visual model for the class of asynchronous algorithms and obtained the first correct conditions of convergence in the nonlinear case for contracting operators.

The following definitions will be used.

Definition A sequence of nonempty subsets $I = \{I_k\}_{k=0}^{\infty}$ of the set {1,2…, m} is a sequence of chaotic sets if $\limsup_{j \to \infty} I_j = \{1,2,...,m\}$. (In other words, if each integer $j \in \{1,2,...,m\}$ appears in this sequence infinite number of times).

Definition If each subset I_k of the sequence of chaotic sets $I = \{I_k\}_{k=0}^{\infty}$ consists of only one element, then such sequence is called acceptable.

Definition A sequence $J = \{\sigma(k)\}_{k=1}^{\infty}$ of *m*-dimensional vectors $\sigma(k) = (\sigma_1(k), \sigma_2(k), ..., \sigma_m(k))$ with the integer coordinates, satisfying the following conditions:

$$0 \le \sigma_i(k) \le k - 1 \tag{21}$$

$$\lim_{k \to \infty} \sigma_i(k) = \infty, \tag{22}$$

for each $i = 1,2,..., m$ and $k \in \mathbf{N}$, is called a sequence of delays.

Let $T = \{T_i\}_{i=1}^m$ be a set of nonlinear operators, acting in the Euclidean space $\mathbf{R}^n$ and let **S** be an algorithmic operator. We will consider the following iterative process:

$$y^{k,i} = T_i x^{(k-1)}, \tag{23}$$

$$x^k = S(x^{(k-1)}, \{y^{k,i}\}_{i=1}^m), \tag{24}$$

where **x** denotes an *n*-dimensional vector of the space $\mathbf{R}^n$ and $i \in \{1,2,...,m\}$, for every k = 0,1,2,.... Then we can formulate one more definition.

Definition Let $\boldsymbol{T}_i$: $R^n \rightarrow R^n$, $i \in \{1,2,...,m\}$ be a set of nonlinear operators and let $\mathbf{x}^{(0)} \in \mathbf{R}^n$ be an initial value of the vector x. A generalized model of the asynchronous iterations with limited delays for the set of operators $\boldsymbol{T}_i$, i=1,2,...,m, is a method of building the sequence of vectors $\{\mathbf{x}^k\}_{k=0}^{\infty}$, which is given recursively by the following scheme:

$$\mathbf{y}^{k,i} = \begin{cases} \mathbf{T}_i \mathbf{x}^{(\sigma^i(k))}, & \text{if } i \in I_k \\ \mathbf{y}^{k-1,i}, & \text{otherwise} \end{cases} \tag{25}$$

$$\mathbf{x}^{(k)} = \mathbf{S}\left(\mathbf{x}^{(k-1)}, \{\mathbf{y}^{k,i}\}_{i \in I_k}\right), \tag{26}$$

where $I = \{I_k\}_{k=1}^{\infty}$ is a sequence of chaotic sets such that $I_k \subset \{1,2,...,m\}$ and $J_i = \{\sigma^i(k)\}_{k=1}^{\infty}$ refer to the sequences of limited delays, for i=1,2,...,m.

Algorithm CHART-3 proceeds according to the following steps:

1. $\mathbf{x}^{(0)} \in \mathbf{R}^n$ is an arbitrary vector;
2. k+1-th iteration is calculated in accordance with following scheme:

$$\mathbf{y}^{k,i} = \begin{cases} \mathbf{P}_i^{\omega_k} \mathbf{x}^{(k-1)}, & \text{if } i \in I_k, \\ \mathbf{y}^{k-1,i}, & \text{otherwise,} \end{cases} \tag{27}$$

$$\mathbf{x}^{(k)} = \mathbf{C} \sum_{i \in I_k} \gamma_i^k \mathbf{y}^{k,i}, \quad (i = 1,2,...,m), \tag{28}$$

where $\mathbf{P}_i^{\omega_k}$ are the operators defined by means of (6) and (8), ω_k denote the relaxation parameters with property $0 < \omega_k < 2$, γ_i^k are the positive real numbers with property:

$$\sum_{i \in I_k} \gamma_k^i = 1, \tag{29}$$

for each $k \in \mathbf{N}$, $I = \{I_k\}_{k=1}^{\infty}$ is the acceptable sequence of chaotic sets such that $I_k \subset \{1,2,...,m\}$ and, finally, $\mathbf{C}$ is the constraining operator. In this paper we consider such $\mathbf{C}$=C_1 C_2 C_3, where:

$$C_1[\mathbf{x}] = \begin{cases} \mathbf{x}, & \text{if } \mathbf{x} \in D, \\ 0, & \text{otherwise,} \end{cases} \tag{30}$$

$$(C_2[\mathbf{x}])_i = \begin{cases} a, & \text{if } x_i < a, \\ x_i, & \text{if } a \le x_i \le b, \\ b, & \text{if } x_i > b, \end{cases} \tag{31}$$

and

$$(C_3[\mathbf{x}])_j = \begin{cases} 0, & \text{if } p_i = 0 \wedge a_{ij} \neq 0, \\ x_j, & \text{otherwise.} \end{cases} \tag{32}$$

3.4. Chaotic-block algorithms

The chaotic and block algorithms, presented in previous sections, can be combined together by forming the chaotic-block algorithms.

New introduced algorithm CHRB-3 runs as follows:

1. $\mathbf{x}^{(0)} \in \mathbf{R}^n$ is an arbitrary vector;
2. k+1-th iteration is calculated in accordance with the following scheme:

$$\mathbf{x}^{k+1} = \mathbf{C} \sum_{i=1}^{M} \mathbf{B}_i^k y^{(k+1),i}, \tag{33}$$

in which the following notation is used:

$$\begin{aligned} y^{(k+1),i} &= \mathbf{Q}_i \mathbf{x}^k, \\ \mathbf{Q}_i &= \mathbf{P}_{i,s_i} \mathbf{P}_{i,s_i-1} ... \mathbf{P}_{i,1}, \\ \mathbf{P}_{i,j} &= \mathbf{P}_j^{\varpi}, \quad j \in I_{i(j)}, \end{aligned} \tag{34}$$

where $\mathbf{P}_i^{\omega}$ refer to the operators defined by relations (6) and (8), symbol $0 < \omega < 2$ describes the relaxation parameters, $\mathbf{C}$ is the constraining operator, $I = \{I_{i(k)}\}_{k=1}^{\infty}$ denotes the sequence of chaotic sets such that $I_{i(k)} \subset \{m_{i-1}+1, m_{i-1}+2, \ldots, m_i\} = H_i$ and $\mathbf{B}_i^k$ are the matrices of dimension $n \times n$, with real nonnegative elements which satisfy conditions (18) and (19), for each $k \in N$.

4. Computer simulation and experimental results

4.1. Problem of the incomplete information

Main of the image reconstruction schemes, depending on system of projections, are parallel and beam schemes are located in the two-dimensional space. In some practical engineering problems, for some important reasons (such as localization, size or limited access to the investigated object), impossible is to get projections from all the directions Such situation arises, for example, in the coal bed working. In the coal bed, during the preparation process, the access to longwalls may be very difficult or impossible at all, in dependence on the method of coal mining. Sometimes it is impossible to access to one or two sides of longwalls, and sometimes it is only impossible to access to the

basis but all the longwalls are accessible. Each of this situation has its own scheme of obtaining the information. In this paper we present the results of the image reconstructions only for two different, the most natural, schemes of obtaining the projection data, which are described below.

In the first scheme, called as the system (1×1), we have an access to the research object from only two opposite sides. This situation often arises in engineering geophysics. In this case the sources of rays are situated only on one side and the detectors are situated on the opposite side of the researched part of, for example, a coal bed. This scheme of obtaining information is shown in Figure 1.

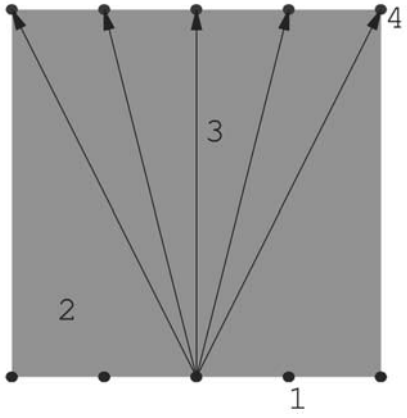

Fig. 1. Scheme of the system (1×1): 1 - sources of rays, 2 - research object, 3 - rays, 4 - detectors

The second scheme of obtaining the projection data, called as the (1×1,1×1) system, is displayed in Figure 2. In this situation we can have an access to all four sides of the examined object. Therefore, the sources can be situated on two neighboring sides, and the detectors can be situated on the opposite sides. In this way, the projections can be obtained from two pairs of the opposite sides.

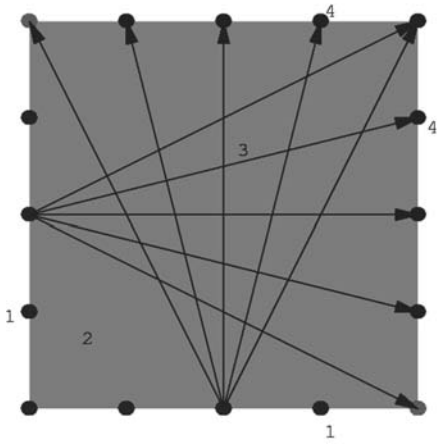

Fig. 2. The system (1×1, 1×1): 1 - sources of rays, 2 - research object, 3 - rays, 4 - detectors

4.2. Models of phantoms

In the simulation process of image reconstruction an important factor is the choice of the density distribution, discrete or continuous, of the researched object. In a coal bed, where we search for the reservoirs of compressed gas or interlayers of a barren rock, the density distribution may be considered as a discrete function and the density difference of these three environments (coal, compressed gas and barren rock) is significant. Therefore, for illustrating the implementation of the algorithms work for the case of incomplete data, we chose the discrete function with high contrast given in the form:

$$f(x,y)=\begin{cases}1, & (x,y)\in D\subset E\subset \mathbf{R}^2,\\ 0, & \text{otherwise},\end{cases} \tag{35}$$

where E is a square $E=\{(x,y):-1\le x,y\le 1\}$ and D is a subset of E of the following form:

D = [-0.4,-0.2] x [-0.5,0.5] $\cup$ [-0.2,0.2] x [0.3,0.5] $\cup$ $\cup$ [-0.2,0.2] x [-0.1,0.1] $\cup$ [0,0.2] x [0.1,0.3].

Another form of the discrete function representing the density distribution can be as is written below:

$$f_1(x,y)=\begin{cases}1, & (x,y)\in D_1\subset E\subset \mathbf{R}^2,\\ 2, & (x,y)\in D_2\subset E\subset \mathbf{R}^2,\\ 3, & (x,y)\in D_3\subset E\subset \mathbf{R}^2,\\ 4, & (x,y)\in D_4\subset E\subset \mathbf{R}^2,\\ 0, & \text{otherwise},\end{cases} \tag{36}$$

where E is a square $E=\{(x,y):-1\le x,y\le 1\}$ and D_i are the following subsets of E

D_1 = [-0.7,-0.4] × [-0.5,0.2],
D_2= [-0.2,0.2] × [-0.1,0.1],
D_3 = [-0.2,0.2] × [0.3,0.5],
D_4 = [0.4,0.7] × [0.4,0.7].

In order to evaluate the good quality of the computed reconstruction of a high-contrast image, from the limited number of projections and incomplete data, we have tested different kinds of geometric figures and reconstruction schemes.

In Figures 3-6 plots of the exemplary functions of density distribution are presented. Those functions are discrete and of high-contrast. Selection of such kind of functions is not accidental, because in technical problems, in which the proposed algorithms can find an application, the density distribution is also discrete and the differences of density between the particular environments are significant. In Figures 3 and 5 the 3D view of the plot of density distribution function is displayed, while in Figures 2 and 4 the 2D view is showed.

Quality of the received reconstruction will be verified by calculating the maximum absolute error:

$$\Delta = \max_i \left| f_i - \tilde{f}_i \right|, \tag{37}$$

the maximum relative error:

$$\delta\% = \frac{\max_i \left| f_i - \tilde{f}_i \right|}{\max_i (f_i)} \cdot 100\%, \tag{38}$$

and the mean absolute error:

$$\delta = \frac{1}{n} \sum_i \left| f_i - \tilde{f}_i \right|, \tag{39}$$

where f_i is the value of the given modeling function in the center of the i-th pixel and $\tilde{f}_i$ is the value of the reconstructed function in the i-th pixel.

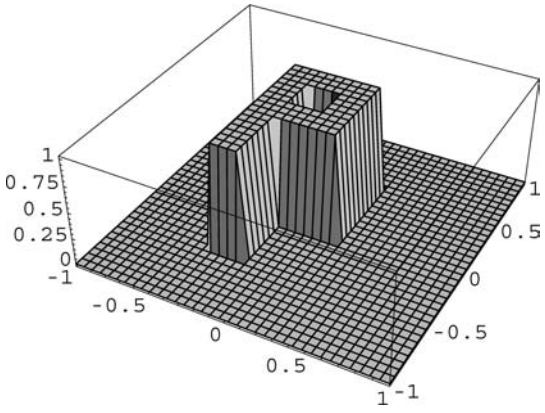

Fig. 3. 3D view of the plot of f

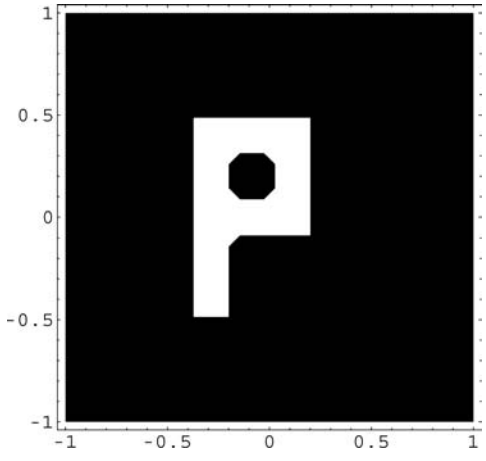

Fig. 4. 2D view of the plot of f (the black color denotes the value 0 and the white color denotes the value 1)

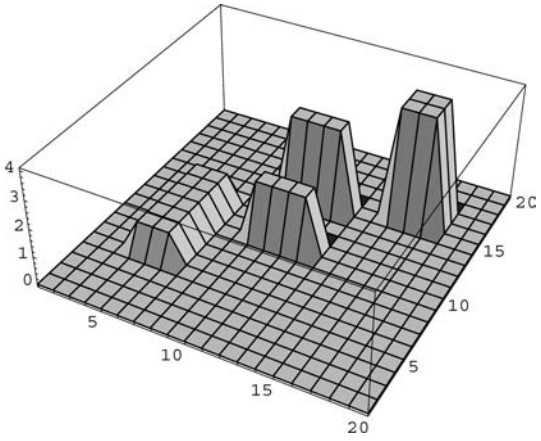

Fig. 5. 3D view of the plot of f_1

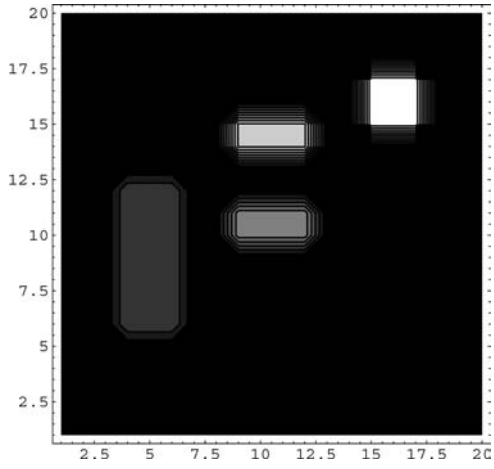

Fig. 6. 2D view of the plot of f_1

4.3. Previous results

Simulations carried out so far indicate that the classical algorithms (ART, ART-3 and MART) are useful for solving the classical problems, as well as the problems of incomplete information. Effectiveness of these algorithms in solving the classical problems has been already proved in several works at the beginning of research concerning the computer tomography. Moreover, their efficiency in regard to the problems of incomplete information is investigated in papers [14,17].

For example, the reconstruction result of $f(x,y)$ with the aid of the algorithm ART-3, after 15 iterations in the reconstruction scheme (1x1,1x1), for n=20 x 20 pixels and for m=644 projections is presented in Figure 7 (where plot of the reconstruction function is displayed) and in Figure 8 (where plot of the mean absolute error for this image reconstruction is showed). Dependence of the mean absolute error and the maximum relative error on the number of iterations for this case of image reconstruction (received by using algorithms ART-3 and CHART-3) is presented in Figures 9 and 10, respectively.

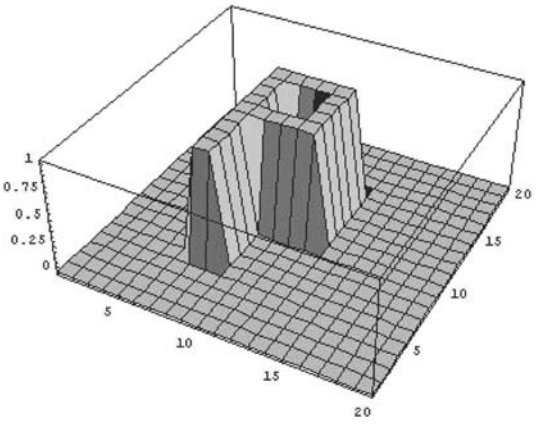

Fig. 7. Plot of the reconstruction of function f

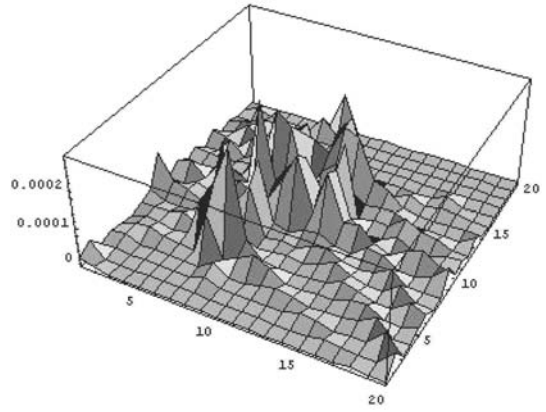

Fig. 8. Plot of the mean absolute errors

Also the non-classical algorithms (SZB-3, BR-3, CHART-3 and CHRB-3) appeared to be convergent and stable in cases of incomplete information. Their effectiveness has been empirically investigated, results of which can be found in [15, 16, 18].

For example, results of the $f_1(x,y)$ reconstruction obtained with the aid of CHRB-3 algorithm, after 500 iterations in the reconstruction scheme (1x1), for n=20 x 20 pixels and for m= 782 projections, is presented in Figure 9 (in which the plot of reconstructed function is displayed) and in Figure 10 (in which the plot of mean absolute error for this image reconstruction is showed).

Carried out experiments [17,18] show that the chaotic algorithms are more useful, in case of each reconstructed function and for every set of reconstruction parameters, than their equivalents which does not apply the randomization. The presented research concerned particularly the problem of incomplete projection data oriented towards some technical applications. However, in the standard approach the chaotic algorithms are also more efficient.

Similarly, by comparing the standard algorithms of computer tomography with the block algorithms it turns out that the block algorithms are more useful (considering the time needed for obtaining the required error, not the number of iterations after which the assumed error is received - do not forget that in the block algorithms we use the simultaneous work of many processors).

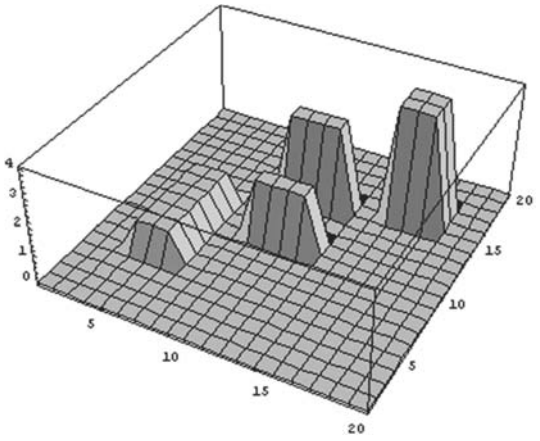

Fig. 9. Plot of the reconstructed function f_1

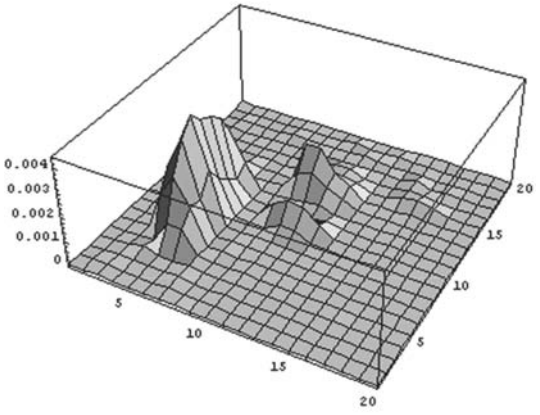

Fig. 10. Dependence of the maximum relative error on the number of iterations for the image reconstruction of f_1 in the system (1x1)

Considering the comparison between two types of block algorithms we suppose to lean towards the RB-3 algorithm. Advantage of this algorithm results from two facts: firstly, because of the technical reasons - in the SZB-3 algorithm one need to use much bigger number of processors than in RB-3 algorithm, secondly, because speed of convergence of algorithm RB-3 is better than in case of algorithm SZB-3.

4.4. Objects with non-transparent elements

In the previous research concerning the usefulness of non-classical computer tomography algorithms for solving non-standard problems of incomplete information the objects containing the non-transparent elements have not been investigated yet. In practice, such situations can be met quite

often. For example, in medicine such case could concern the examination of patient who has in his body some pieces of metal (like a needle, a shrapnel, a golden tooth or a swallowed coin). In medicine this classical problem is already solved. Whereas, the cases of incomplete information (expressed in form like considered in this paper) have not been investigated yet, either for classical or non-classical algorithms. In suggested applications of those algorithms (in mining industry, for example) the non-transparent elements could be the objects lying in the coal interlayer and having strictly higher capacity to absorb energy than coal, stones or compressed gas, usually lying in coal interlayers. The objects with non-transparent elements will be modeled by using the modified functions f and f_1.

Such modification is formulated by the relation (40) corresponding to function f:

$$g(x,y)=\begin{cases}1, & (x,y)\in D\subset E\subset \mathbf{R}^2,\\ M, & (x,y)\in D_1\subset E\subset \mathbf{R}^2\\ 0, & \text{otherwise,}\end{cases} \tag{40}$$

where E denotes a square $E=\{(x,y):-1\le x,y\le 1\}$, D is a subset of E having the following form:

D = [-0.4,-0.2] x [-0.5,0.5] $\cup$ [-0.2,0.2] x [0.3,0.5] $\cup$ $\cup$ [-0.2,0.2] x [-0.1,0.1] $\cup$ [0,0.2] x [0.1,0.3] ,

D_1 is a subset of E such that $D\cap D_1=\varnothing$ and M refers to a constant such that $M>>1$. Similar modification but corresponding to function f_1 is given by the relation (41):

$$g_1(x,y)=\begin{cases}1, & (x,y)\in D_1\subset E\subset \mathbf{R}^2,\\ 2, & (x,y)\in D_2\subset E\subset \mathbf{R}^2,\\ 3, & (x,y)\in D_3\subset E\subset \mathbf{R}^2,\\ 4, & (x,y)\in D_4\subset E\subset \mathbf{R}^2,\\ M, & (x,y)\in D_5\subset E\subset \mathbf{R}^2,\\ 0, & \text{otherwise,}\end{cases} \tag{41}$$

where E denotes a square $E=\{(x,y):-1\le x,y\le 1\}$, D_i are the subsets of E of the following form:

D_1 = [-0.7,-0.4] × [-0.5,0.2], D_2= [-0.2,0.2] × [-0.1,0.1],

D_3 = [-0.2,0.2] × [0.3,0.5], D_4 = [0.4,0.7] × [0.4,0.7],

D_5 is a subset of E such that for each $0<i<5$ there is $D_5\cap D_i=\varnothing$ and M refers a constant such that $M>>4$.

Value of the constant M is finite for the need of graphic presentation of the considered function with non-transparent element. In reality and in carried out simulations we have $M=\infty$, that is the non-transparent element absorbs the entire energy of the ray hitting this element. It means that each projection, with the non-transparent element on its road, does not carry any information, except the one informing about the existence of some non-transparent element in some unknown place.

We assume in the paper that the non-transparent elements are determined in the discs of given centre and radius, which means that the set D_1 or D_5 are of the form $\{(x,y):(x-x_0)^2+(y-y_0)^2\le r^2\}\subset E$. Exemplary model of such object is showed in Figure 11.

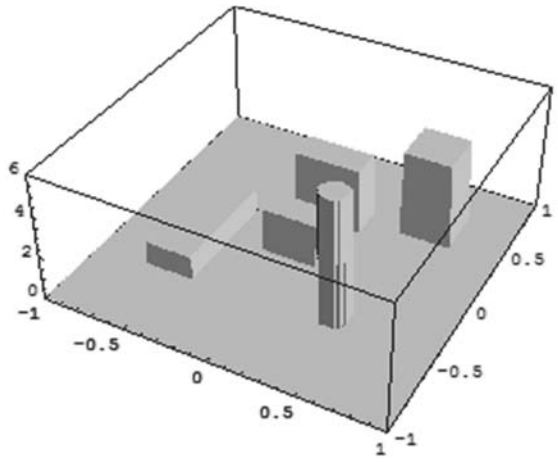

Fig. 11. Example of the object defined by means of function g_1 with the non-transparent element

4.5. Efficiency of the classical algorithms in examining the objects with non-transparent elements

In this section we present a discussion of efficiency of the classical algorithms ART, ART-3 and MART in examining the objects with non-transparent elements. The research are made on the assumption of incomplete set of data - such problem has been presented in Section 4.1. Moreover, the research is carried out for functions $g(x,y)$ and $g_1(x,y)$ describing the density distribution of examined objects.

In the current paper only these regions of domain of functions $g(x,y)$ and $g_1(x,y)$ will be reconstructed in which the functions take finite value (it means, we reconstruct the corresponding functions $f(x,y)$ and $f_1(x,y)$). Determination of the precise location of the non-transparent elements will be a subject of the next work.

Figures 12 and 13 present the examined density distribution functions $g(x,y)$ and $g_1(x,y)$ where the non-transparent elements (sets D_1 and D_5, respectively) are disks: $(x-0.2)^2+(x+0.6)^2\le(0.05)^2$ and $(x-0.4)^2+(x+0.4)^2\le(0.09)^2$, respectively.

In Figures 14-19 the results of work of the MART algorithm are displayed, for the system (1×1,1×1), functions $g(x,y)$ and $g_1(x,y)$ and for the proper values of the following parameters: number of sources on one side m, discretization density of reconstructed object n (number of pixels $N=n^2$), iteration number *iter*, together with plots of these reconstruction errors.

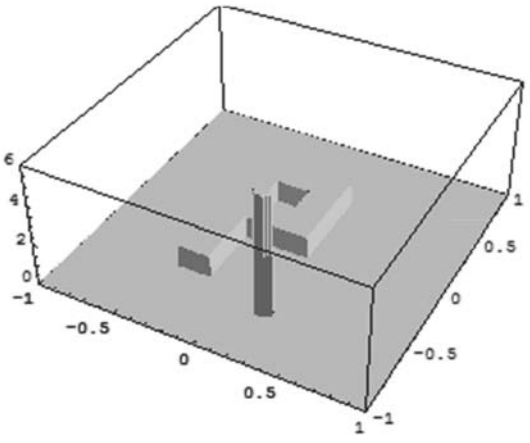

Fig. 12. Reconstructed function *g(x,y)*

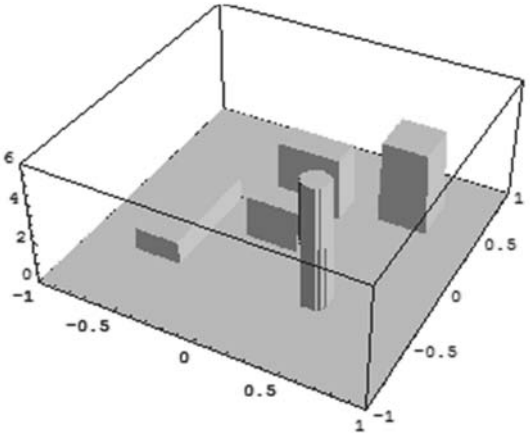

Fig. 13. Reconstructed function $g_1(x,y)$

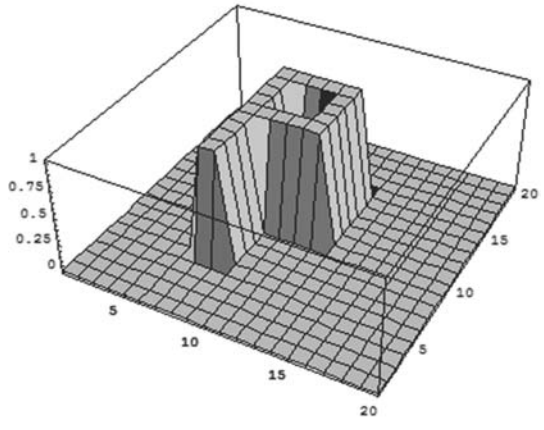

Fig. 14. Reconstruction of function *g(x,y)* (3D view) for *m*=30, *n*=20, *iter*=50, in system (1×1, 1×1)

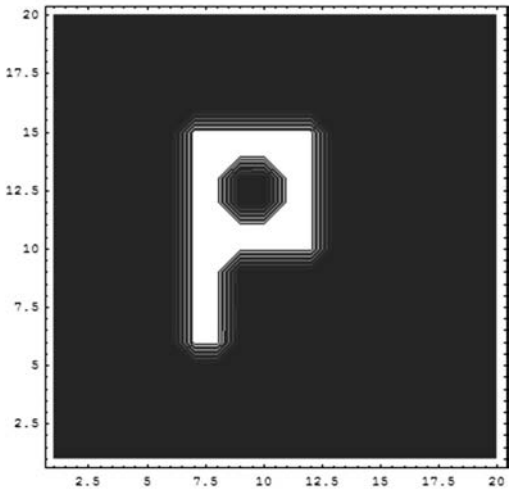

Fig. 15. Reconstruction of function *g(x,y)* (2D view) for *m*=30, *n*=20, *iter*=50, in system (1×1,1×1)

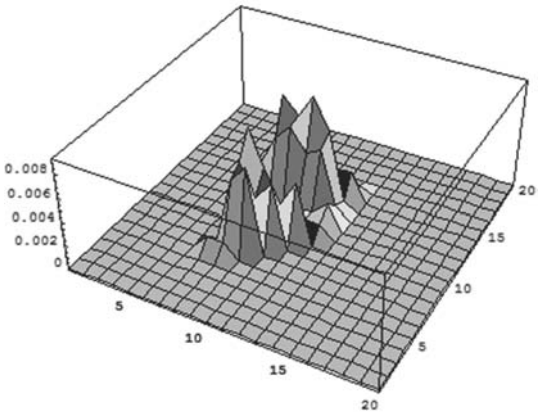

Fig. 16. Plot the absolute errors | *g(x,y)* –*ğ(x,y)* for *m*=30, *n*=20, *iter*=50, in system (1×1,1×1)

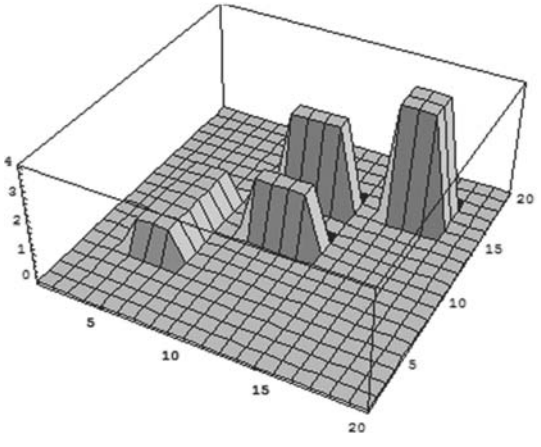

Fig. 17. Reconstruction of function $g_1(x,y)$ (3D view) for *m*=30, *n*=20, *iter*=50, in system (1×1,1×1)

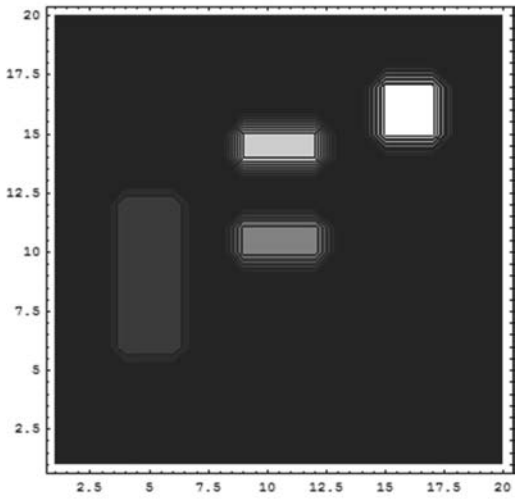

Fig. 18. Reconstruction of function $g_1(x,y)$ (2D view) for m=30, n=20, *iter*=50, in system (1×1,1×1)

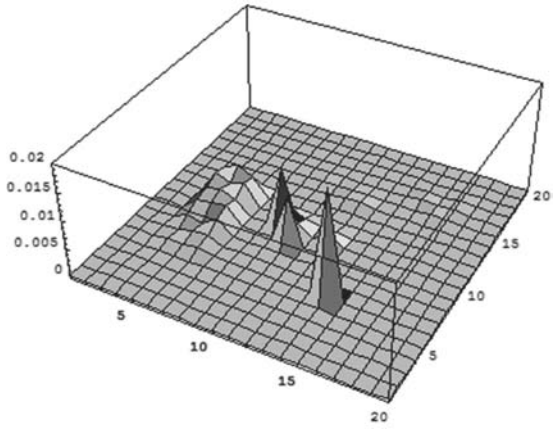

Fig. 19. Plot the absolute errors $|g_1(x,y) - \check{g}_1(x,y)|$ for m=30, n=20, *iter*=50, in system (1×1,1×1)

For the case of system (1×1) the exemplary reconstructions are showed in Figures 20-23.

Presented reconstructions represent only the examples. Cases with various qualities of reconstruction are showed in purpose. Series of the carried out experiments indicate that for each of the examined density distribution functions, for each system and for the non-transparent elements located in "reasonable" way (the elements are disjoint with sets D_i - problem of intersections will be considered in next papers - and they are of not too big sizes), for each resolution (value of parameter n) there exists such values of parameters m and *iter* that the received reconstruction is of the desired quality. For example, in Figures 24 and 25 the errors of reconstructions generated with the aid of algorithms ART and ART-3 are displayed (additionally, in the first case the non-transparent element is located in the bowl of letter P).

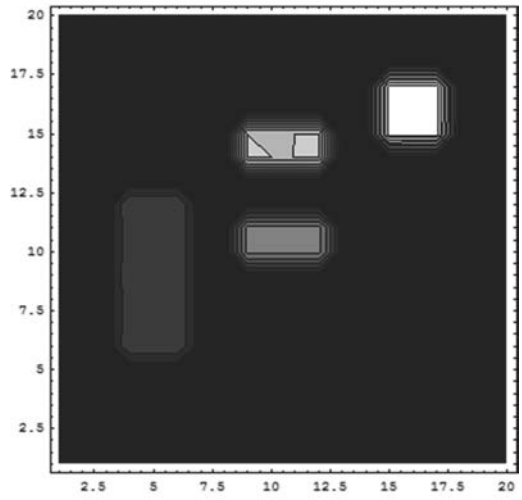

Fig. 20. Reconstruction of function $g_1(x,y)$ (2D view) for m=18, n=20, *iter*=250, in system (1×1)

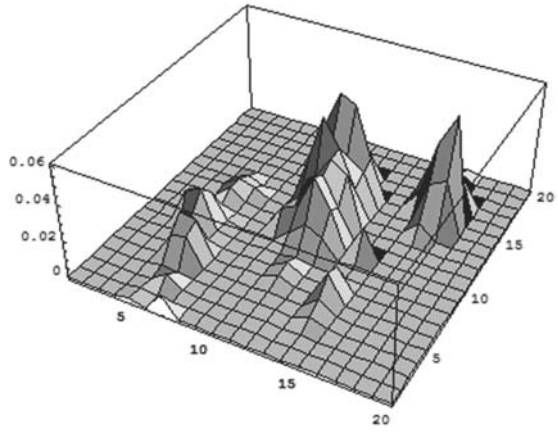

Fig. 21. Plot the absolute errors $|g_1(x,y) - \check{g}_1(x,y)|$for m=18, n=20, *iter*=250, in system (1×1)

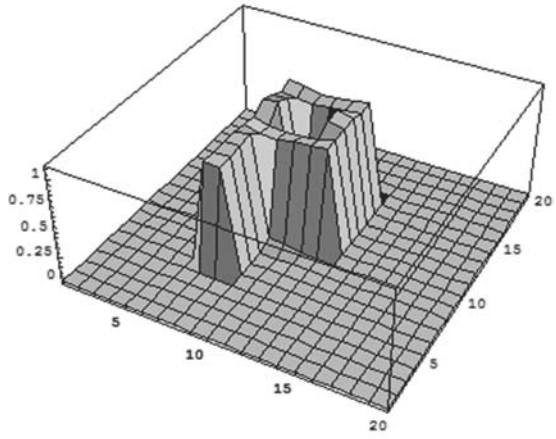

Fig. 22. Reconstruction of function $g(x,y)$ (3D view) for m=18, n=20, *iter*=250, in system (1×1)

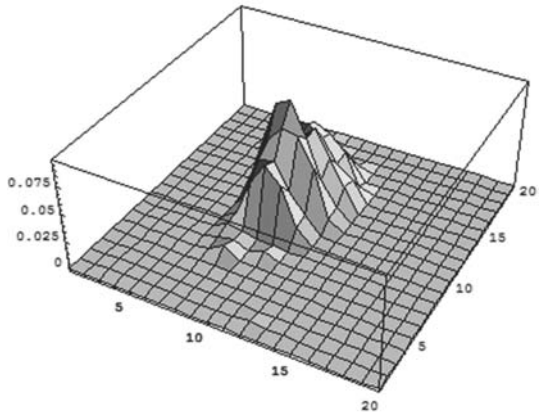

Fig. 23. Plot the absolute errors $|g(x,y) - \check{g}(x,y)|$ for m=18, n=20, *iter*=250, in system (1×1)

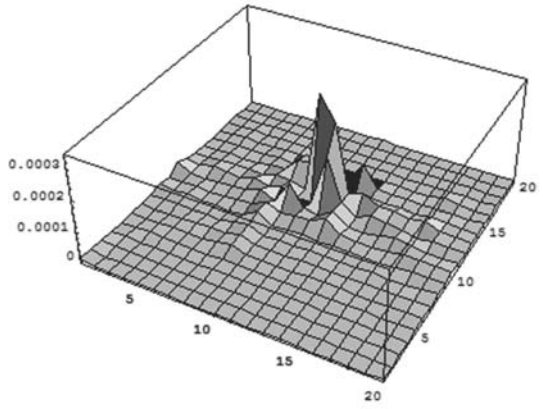

Fig. 24. Plot the absolute errors $|g(x,y) - \check{g}(x,y)|$ for m=18, n=20, *iter*=25, in system (1×1,1×1), for set $D_1 = (x + 0.1)^2 + (x - 0.2)^2 \leq (0.05)^2$

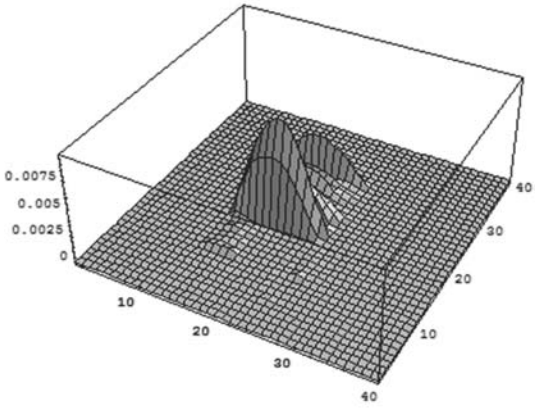

Fig. 25. Plot the absolute errors $|g(x,y) - \check{g}(x,y)|$ for m=58, n=40, *iter*=500, in system (1×1), for set $D_1 = (x - 0.2)^2 + (x + 0.6)^2 \leq (0.05)^2$

4.6. Efficiency of the non-classical algorithms in examining the objects with non-transparent elements

In this section the effectiveness of non-classical algebraic algorithms (introduced in Section 3) in examination of the objects with non-transparent elements is investigated. The research is realized on the assumption of incomplete set of data which is presented in Section 4.1 and, similarly like in previous case, the research is made for functions $g(x,y)$and $g_1(x,y)$ describing the density distribution of examined objects.

In algorithms discussed in this section, in most of cases the projection matrix **A** is divided into blocks for the purpose of possibility to parallelize the calculations. Such division depends, in natural way, on the number of rays sources - each source generates some beam of rays which can determine a certain block. Vector of solutions after the full iteration is defined by the weighted mean of the partial solutions vectors received from every block. In case when the non-transparent element is located nearby the source or when the non-transparent element is of the large size, some blocks will exist such that most of the projection will be absorb by this element, which means that the solution vector from this block will falsify the total image. That is why some modifications of algorithms SZB-3, RB-3 and CHRB-3 are needed thanks to which they will be more efficient. The mentioned modification will be a subject of further research.

Algorithm which do not need any modification is CHART (or CHART-3). Reconstruction results obtained with the aid of this algorithm are presented in the next figures.

Figure 26 shows the absolute error of reconstruction similar to those one presented in Figure 24. The results indicate that, similarly as in cases of objects without non-transparent elements, the chaotic algorithm is more useful, for the same values of parameters, in comparison with the corresponding algorithms. The reconstruction errors are three times smaller than the errors received for algorithm ART-3.

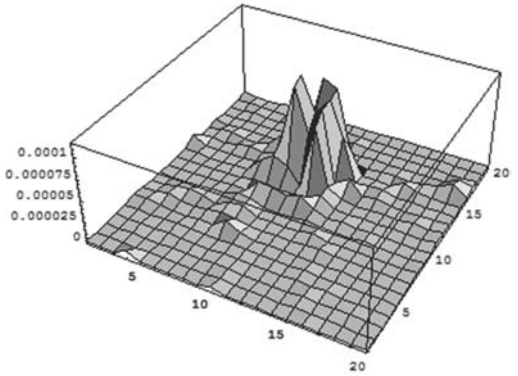

Fig. 26. Plot the absolute errors $|g(x,y) - \check{g}(x,y)|$ for CHART-3 algorithm, for parameters m=18, n=20, *iter*=25, in system (1×1,1×1), for set $D_1 = (x + 0.1)^2 + (x - 0.2)^2 \leq (0.05)^2$

Whereas, in Figure 27 the absolute error of reconstruction similar to those one presented in Figure 25 is showed. Again, it turned out that the chaotic algorithm is more efficient than the corresponding ART algorithm.

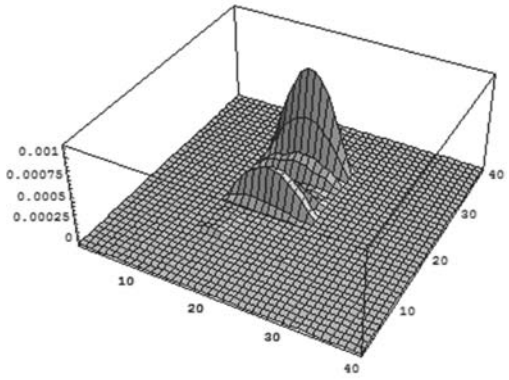

Fig. 27. Plot the absolute errors $|g(x,y) - \check{g}(x,y)|$ for CHART-3 algorithm, for parameters m=58, n=40, $iter$=500, in system (1×1), for set $D_1 = (x - 0.2)^2 + (x + 0.6)^2 \leq (0.05)^2$

5. Conclusions

In this paper we have presented the number of computer tomography algorithms, known from the literature and designed by the authors, applied in the standard approach or, after the proper adaptation, in solving the problems of the incomplete projection data and in reconstructing the objects with non-transparent elements. We have considered the general model of asynchronous iterations and new block, chaotic and chaotic-block iterative algorithms for reconstruction of the high-contrast objects from incomplete projection data, without and with the non-transparent elements. These algorithms can be realized on the parallel computing structure consisting of elementary processors and some central processor, all of which are connected with shared memory.

The effectiveness and convergence of presented algorithms have been discussed. The experimental results show that convergence of the block-parallel chaotic algorithm CHRB-3 is better by comparison with the block-parallel algorithm RB-3, the iterative-block algorithm SZB-3 and especially with standard algorithms. Moreover, discussion of efficiency of the classical algorithms ART, ART-3 and MART, as well as the non-classical algorithms, in examining the objects with non-transparent elements in condition of the incomplete set of data confirmed this conclusion. Showed results indicate that, similarly as in cases of objects without non-transparent elements, the chaotic algorithms are more efficient, for the same values of parameters, in comparison with the corresponding classical algorithms.

Taking into account the time of implementation, for the block-parallel algorithm implemented on multiprocessors computers the time is approximately M times smaller (where M is the number of processors which is equivalent to the number of blocks) than for the sequential computers. Additionally, from results of computer simulation it follows that the time of running of the block-parallel algorithms is better with comparison with the sequential ART-3.

Another conclusion resulting from presented research is that the configuration (1×1,1×1) is considerably better by comparison with the scheme (1×1). And for each considered scheme of reconstruction there exist the parameters which allow to obtain the enough good quality of reconstruction after some number of iterations but this number is considerably larger than for reconstruction with complete projection data. However, in some technical problems (like for example in examining the coal bed where the access to the researched object is significantly limited - see the Figure 1) it is impossible to use the scheme (1×1,1×1). The received results indicate that the discussed algorithms are convergent also for the system (1×1), but for receiving the same reconstruction quality they need the considerably bigger number of iterations. Moreover, all the considered algorithms are stable.

References

[1] D. Patella, Introduction to ground surface self-potential tomography, Geophysical Prospecting 45 (1997) 653-681.
[2] R.A. Williams, K. Atkinson, S.P. Luke, R.K. Barlow, B.C. Dyer, J. Smith, M. Manning, Applications for tomographic technology in mining, minerals and food engineering, particle and particle systems characterization 12 (2004) 105-111.
[3] A.H. Andersen, Algebraic Reconstruction in CT from limited views, IEEE Transactions on Medical Imaging 8 (1989) 50-55.
[4] H. Guan, R. Gordon, Computed tomography using algebraic reconstruction techniques with different projection access schemes: a comparison study under practical situation, Physics in Medicine and Biology 41 (1996) 1727-1743.
[5] M.R. Trummer, A note on the ART of relaxation, Computing 33 (1984) 349-352.
[6] Y. Censor, Parallel optimization: theory, Algorithms, and Applications, New York Oxford Oxford University Press, 1997.
[7] G.M. Baudet, Asynchronous iterative methods for multiprocessors, Journal of the Association for Computing Machinary 25 (1978) 226-244.
[8] D.P. Bertsekas, J.N. Tsitsiklis, Parallel and Distributed Computation: Numerical Methods. Prentice-hall, Englewood Cliffs, NJ, 1989.
[9] D. Chazan, W. Miranker, Chaotic relaxation, Linear Algebra and Its Applications 2 (1969) 199-222.
[10] Y. Censor, Parallel application of block-iterative methods in medical imaging and radiation therapy, Mathematical Programming 42 (1988) 307-325.
[11] A.R. De Pierro, A.N. Iusem, A parallel projection method of finding a common point of a family of convex sets, Pesquisa Operacional 5 (1985) 1-20.
[12] R. Bru, L. Elsner, M. Neumann, Models of parallel chaotic iteration methods, Linear Algebra and Its Applications 103 (1988) 175-192.
[13] N. Gubareni, Computed methods and algorithms for computer tomography with limited number of projection data, Naukova Dumka, Kiev, 1997 (in Russian).
[14] N. Gubareni, M. Pleszczyński, Image reconstruction from incomplete projection data by means of iterative algebraic algorithms, Proceedings of the International Multi-conference on Computer Science and Information Technology, Wisła, 2007.
[15] N. Gubareni, M. Pleszczyński, Chaotic iterative algorithms for image reconstruction from incomplete projection data, Electronic Modelling 30 (2008) 29-43.

[16] N. Gubareni, M. Pleszczyński, Block-parallel chaotic algorithms for image reconstruction, Electronic Modeling 31 (2009) 41-54.
[17] M. Pleszczyński, Badanie efektywności algorytmów rekonstrukcyjnych tomografii komputerowej przy niepełnym zbiorze danych, praca doktorska, Częstochowa, 2009.
[18] R. Grzymkowski, E. Hetmaniok, M. Pleszczyński, A. Zielonka, Application of the computer tomography in examination of the internal structure of materials by considering the specific conditions of the problem, Journal of Achievements in Materials and Manufacturing Engineering 43/1 (2010) 288-298.
[19] M.N. El Tarazi, Algorithmes mixtes asynchrones, Etude de la convergence monotone, Numerische Mathematik 44 (1984) 363-369.
[20] S. Helgason, The radon transform, Springer-Verlag, 1999.